15 Pharmacokinetic Data Analysis and Modeling of ADME Processes

STEVEN ZHANG

Department of Clinical Pharmacology and Pharmacometrics, Bristol-Myers Squibb, Princeton, NJ, USA

15.1 INTRODUCTION

Human absorption, distribution, metabolism, and elimination (ADME) studies are routinely conducted for small molecule drug candidates mostly during the stage of early clinical development to characterize their ADME in the body. Since biological drug candidates, in general, contain only the naturally occurring components of amino acids or nucleic acids, there is no need to perform a human ADME study to understand metabolism and/or elimination for these drug candidates. However, a human ADME study may be desirable for the biological drug candidates that contain chemically modified components such as unnatural amino acids, nucleic acid analogs, or antibody–drug conjugate with small molecule chemical drug complexes.

Pharmacokinetic (PK) evaluation in human ADME study is intended to define the systemic exposure of a drug and its metabolite(s), in particular, pharmacologically active metabolites in the body after dose administration. The most important information of drug and/or metabolite concentration–time profile is to provide the rate and extent of ADME.

Plasma and urine data obtained in human ADME studies can be used to calculate standard PK parameters for unchanged drug, such as time of maximum observed plasma concentration (T_{max}), maximum observed plasma concentration (C_{max}), area under the plasma concentration–time curve from time zero to infinite time ($AUC_{0-\infty}$) or to time of last quantifiable concentration (AUC_{last}), clearance (CL), volume of distribution (V), elimination half-life ($t_{1/2}$), renal clearance (CL_R), and percentage of dose excreted

Encyclopedia of Drug Metabolism and Interactions, 6-Volume Set, First Edition.
Edited by Alexander V. Lyubimov.

unchanged in urine. These PK results confirm appropriateness of ADME study design and study conductivity if these results are comparable with the results for the same drug from other previously conducted phase I trials.

To date, two different methods have been used to analyze drug and metabolite kinetics. The first is noncompartmental analysis (NCA), also called *model-independent analysis* of concentration–time profile. This model is not necessarily restricted to the assumption of compartments and is a simple first-order distribution or elimination process. The second approach is compartmental analysis and utilizes mathematical models to describe drug/metabolite behavior in the body, with assumptions of well-mixed compartments and following certain mathematical equations. With the limited assumptions required, NCA allows the estimation of the most basic PK parameters characterizing the ADME processes of a drug. NCA methods are relatively simple to use prevailing in drug development and regulatory evaluation. Nearly all PK analysis of phase I intensive data are completed using NCA. Although NCA provides useful summary assessments of PK parameters, it does not provide some important PK parameters such as rate constants and distribution of drug to different compartments that could help researchers understand mechanisms of drug disposition and action. On the other hand, the mechanistic, model-dependent approach can provide information for a more quantitative understanding of drug action in living cells, organisms, or disease-related targets. Considering that drug development is an information-gathering process of learn–confirm cycles, mechanistic modeling plays an important role in knowledge-based drug development and eventually regulatory approval.

In addition to identifying the major excretory pathways, much can be learned from ADME studies about blood, bile, urine, and feces data of unchanged drug and total radioactivity (TRA). The goal of this chapter is to demonstrate how important information relating to drug ADME may be obtained from the analysis of PK data. The theory and application of PK data analysis and modeling to characterize the PK of a drug and its metabolite(s) based on blood and urine data are presented. The discussion focuses on conventional methods that have been utilized in assessing PK data in human studies.

15.2 RECOVERY OF THE RADIOACTIVE DOSE IN EXCRETA

One of the objectives of a human ADME study is to evaluate mass balance of an administered drug. This type of study provides information on the amount of drug that is recovered over time via the different elimination routes of the body after dose administration. The analyses of radioactivity in excreta sample such as urine, feces, and bile offer information regarding elimination routes of the drug. In human ADME studies, the cumulative excreta samples of urine and feces across the entire study period in each subject are collected following a single oral or intravenous (IV) administration of a radiolabeled drug. For some orally administered drugs, bile samples may also be collected if biliary excretion is expected to be a major route for elimination of drug or its direct conjugates/unstable metabolites that will be converted back to the parent by hydrolysis of the conjugate in the gut microflora. With these samples analyzed, the recovery of the radioactive dose in excreta can be estimated.

It is ideal to have mass balance, that is, near complete recovery with at least 90% of the total administered radioactivity recovered in excreta. A case study using a

Bristol-Myers Squibb drug candidate (BMS-690514) is used as an example of a typical human ADME study and also used to discuss noncompartmental PK data analysis later in this chapter. In the human ADME study of [^{14}C]BMS-69051 [1], an orally administered selective inhibitor of human epidermal growth factor receptors (HERs) and vascular endothelial growth factor receptors (VEGFRs), a single 200-mg dose of [^{14}C]BMS-690514 containing 80 μCi of radioactivity (0.39 μCi/mg) in a solution of 50 m*M* citric acid was administered orally to a total of nine healthy male subjects, who were randomly assigned to group 1 ($n = 6$) without bile sample collection or to group 2 ($n = 3$) with bile sample collection. The blood, urinary, and fecal samples were collected up to 216 h postdose and bile samples were obtained from 3 to 8 h postdose by positioning the terminal end of an oral gastroduodenal tube at the vertical limb of the duodenal loop near the ampulla of Vater (confirmed via fluoroscopy). The TRA in excreta was determined by liquid scintillation counting and the concentration of drug-derived ^{14}C radioactivity in individual plasma samples was determined by accelerator mass spectrometry. Following oral administration of [^{14}C]BMS-690514, the mean cumulative recovery of radioactivity over the 0- to 264-h collection interval was 99.98% (Fig. 15.1). The majority of radioactivity, 50%, was recovered in the feces and ~34% was recovered in the urine. For subjects with bile collection, an additional 16% of the dose was recovered in the bile over the 3- to 8-h postdose interval. The excretion rate reached a plateau at 96 h postdose with <2% daily incremental changes thereafter.

Although there are many ways to increase the chance to achieve a high recovery such as by preventing a labeled fragment of the drug from entering endogenous compound metabolism and prohibiting conversion of the label to a volatile metabolite, it is not unusual to obtain <100% recovery of the radiolabeled dose in a mass balance study. Beumer *et al*. [2] suggest that total recovery should be at least 90% of the

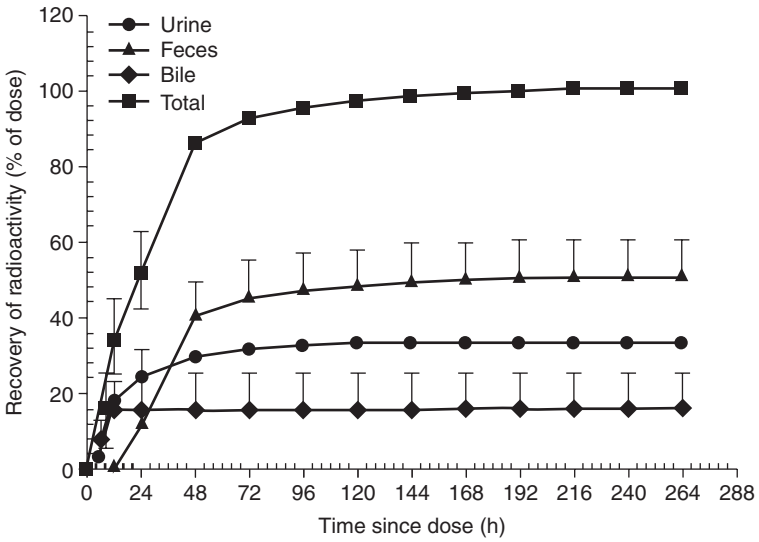

Figure 15.1 Mean ± SD cumulative recovery of radioactivity after administration of a single 200-mg (80-μCi) PO dose of [^{14}C]BMS-690514 to healthy male subjects—time course for excretion of radioactivity in urine, faces, bile, and total excreta [1].

administered dose with a 10% margin ($100 \pm 10\%$) as being acceptable. Roffey *et al*. [3] reviewed 171 human mass balance studies and found that 42% had overall recovery values below 90%. If the criteria were dropped to 80%, 15% of mass balance studies would have been considered failures. Low recovery of radioactivity can be explained by biological factors such as binding to specific proteins in tissues, binding to melanin, binding to phospholipids, and covalent and noncovalent binding to tissue. Noncompliance by subjects/study personnel to meticulously collect all excreta samples can also contribute to a low recovery. In general, the drugs with a long half-life tend to show low recovery of administered radioactivity. The success or failure of a mass balance study is dependent on the value of absolute recovery. The acceptance of a mass balance study is ultimately based on achievability of the primary objective of human mass balance study to determine the profile of parent drug and metabolites using excretory and circulatory samples obtained in this study.

15.3 PHARMACOKINETIC ANALYSIS OF BLOOD DATA USING NONCOMPARTMENTAL ANALYSIS

Typically, serial blood samples are collected after single-dose administration of radiolabeled drug in order to characterize the PK of TRA and the drug from plasma or serum concentration versus time profiles in human ADME studies. This allows pharmacokinetists to determine the PK parameters of TRA and a drug by an NCA method without the assumptions of mixed compartments and following certain mathematical equations.

The single-dose PK parameters assessed in human ADME studies, in general, include T_{max}, C_{max}, AUC_{last}, $AUC_{0-\infty}$, $t_{1/2}$, CL/F (apparent total body clearance), and V_{ss}/F (apparent steady-state volume distribution) for an orally administered radiolabeled drug. If a radiolabeled drug is administered via IV injection, the same set of PK parameters will be estimated as for an oral drug, except absolute CL and V_{ss} will be estimated.

The C_{max} and T_{max} are obtained from experimental observations. The terminal log-linear phase of the concentration–time curve is identified by least-square linear regression of at least three data points that yielded a maximum G-criterion, which is also referred to as *adjusted* R^2, using no weighting factor. The $t_{1/2}$ value was calculated as $Ln2/k_{el}$, where k_{el} was the absolute value of the slope of the terminal log-linear phase. The AUC_{0-T} was calculated using the mixed log-linear trapezoidal algorithm with a NCA method. The $AUC_{0-\infty}$ was estimated by summing AUC_{0-T} and the extrapolated area, computed by the quotient of the last observable concentration and k_{el}.

As an example, the mean plasma concentration–time profiles and PK parameters for TRA and BMS-690514 are shown in Fig. 15.2 and Table 15.1, respectively. BMS-690514 was rapidly absorbed with T_{max} values ranging from 0.5 to 2 h postdose. T_{max} values for TRA occurred between 1.5 and 4.0 h postdose and reflected a composite plasma concentration–time profile of BMS-690514 and other metabolites in plasma. On the basis of the $AUC_{0-\infty}$ values, the unchanged parent drug, BMS-690514, accounted for ~3.2% and 7.6% of the circulating radioactivity in group 1 (without bile sample collection) and group 2 (with bile sample collection) subjects, respectively, suggesting that metabolites contributed significantly to the circulating radioactivity. Plasma TRA

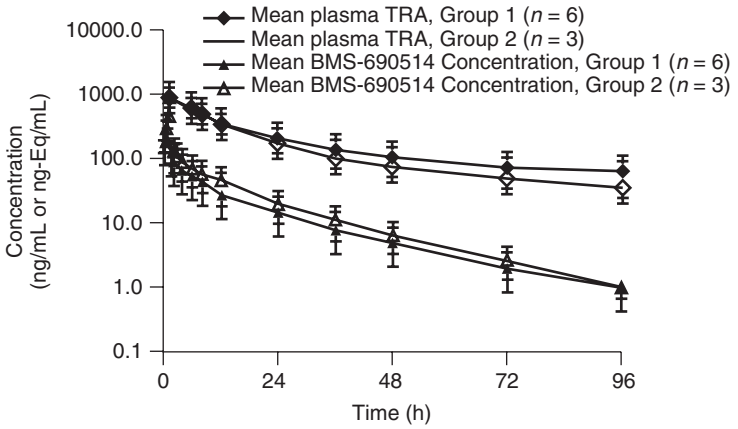

Figure 15.2 Mean ± SD plasma concentration–time profile for total radioactivity (TRA) and BMS-690514. Concentrations of drug-derived radioactivity in plasma were determined by accelerator mass spectrometry (AMS); BMS-690514 concentrations were measured with a validated LC-MS/MS assay [1].

was eliminated from the systemic circulation at a slower rate than parent drug, which had a mean $t_{1/2}$ of 16.7 h for the two groups combined. Subjects who went through bile collection had generally lower systemic exposures to TRA than those who did not have bile collection.

15.4 PHARMACOKINETIC ANALYSIS OF URINE DATA

Since renal excretion is an important route of elimination for many drugs, analysis of urinary data can provide useful PK information. Although urine data are less reliable than plasma or serum data for the calculation of PK parameters, together with plasma or serum data, they may allow the calculation of renal clearance. The ratio of a drug excreted unchanged to the TRA excreted in urine is also informative. Comparison of this ratio to the ratio of an unchanged drug to the TRA in plasma or serum may generate insight into drug–metabolite differences in passive/active excretion and reabsorption in the kidneys.

15.4.1 Renal Clearance

Renal excretion is an important route of elimination for many drugs, including unchanged drugs that are primarily excreted in urine and many drug metabolites that are formed by hepatic metabolism of the parent drug. Renal clearance, a useful PK parameter, can be calculated from analysis of urinary data together with plasma data obtained in the human ADME study.

Renal clearance is the hypothetical volume of plasma from which the substance is eliminated by the kidney appearing in the urine per unit time. A physiologic definition of renal clearance (CL_R) is a ratio of the instantaneous urinary

TABLE 15.1 Pharmacokinetic Parameters of Total Radioactivity and BMS-690514 After a Single 200-mg PO Dose of [^{14}C]BMS-690514 to Healthy Subjects in Group 1 (without Bile Collection) and Group 2 (with Bile Collection)

	BMS-690514					Total Radioactivity			
	T_{max} (h)	C_{max} (ng/mL)	$AUC_{(INF)}$ (ng h/mL)	$t_{1/2}$ (h)	UR (%)	T_{max} (h)	C_{max} (ng Eq/mL)	$AUC_{(INF)}$ (ng Eq/mL)	$t_{1/2}$ (h)
Group 1 ($n = 6$)	0.5 (0.5, 1.0)	173.55 (44)	1205.07 (37)	15.98 ± 2.31	2.97 ± 0.83	2.01 (1.50, 4.00)	913.41 (23)	37,579.68 (45)	327.14 ± 287.78
Group 2 ($n = 3$)	0.52 (0.45, 2.12)	142.49 (26)	1698.52 (10)	18.13 ± 2.22	4.19 ± 1.14	2.12 (1.92, 4.00)	724.33 (18)	22,246.77 (28)	170.46 ± 72.36
All ($n = 9$)	0.5 (0.45, 2.12)	162.52 (38)	1351.13 (31)	16.70 ± 2.39	3.37 ± 1.06	2.02 (1.50, 4.00)	845.45 (24)	31,554.24 (49)	274.92 ± 243.33

Data are presented as median (minimum, maximum), geometric mean (percent coefficient of variance), or mean ± SD.

excretion rate (dA_e/dt) and the plasma concentration of drug at the time when the urinary sample is collected (C_p):

$$CL_R = \frac{dA_e/dt}{C_p} \tag{15.1}$$

This equation assumes that urine is collected over a finite period during which the plasma concentration of drug is changing following first-order kinetics. Practically, renal clearance is calculated as the ratio of the amount of drug excreted unchanged ($A_{e(\Delta t)}$) during a urine collection interval (Δt) to the plasma concentration of drug at the midpoint of the interval (C_{mid}):

$$CL_R = \frac{A_{e(\Delta t)}/\Delta t}{C_{mid}} \tag{15.2}$$

By rearranging Equation 15.2, the slope of a linear regression of multiple urine collections ($A_{e(\Delta t)}/\Delta t$) versus C_{mid} is equal to average renal clearance. A short collection period approximates the change in plasma concentration of drug linearly with time but increases the inaccuracy in the estimate of excretion rate due to incomplete bladder emptying. On the other hand, prolonging the urine collection interval can avoid the problem of incomplete emptying. However, the change in drug plasma concentration during a sample collection interval may no longer follow a linear function because the drug plasma concentration is in fact changing exponentially with time under the conditions of Equation 15.1. In practice, a lower limit and upper limit for a collection interval, dt in Equation 15.1 and Δt in Equation 15.2 is ~0.5 h [4] or less than an elimination half-life [5].

When taking integration of Equation 15.1 from time 0 to infinity, the numerator dA_e becomes $A_{e(\infty)}$ and the denominator $C_p dt$ is the corresponding area under the plasma concentration–time curve of drug ($AUC_{0-\infty}$):

$$CL_R = \frac{A_{e(\infty)}}{AUC_{0-\infty}} \tag{15.3}$$

Clinically, severe difficulties with compliance in plasma and urine sample collection may occur, especially for drugs with a long terminal elimination half-life as typically a sample collection period of at least five terminal elimination half-lives can be considered to be equivalent to infinite term. Equation 15.3 is practically modified as follows:

$$CL_R = \frac{A_{e(t_2-t_1)}}{AUC_{(t_2-t_1)}} \tag{15.4}$$

On the basis of the plasma and urine data obtained in a human ADME study as presented in Table 15.2 and Figs. 15.3 and 15.4, renal clearance of a drug can be calculated by applying Equation 15.2 or 15.3. The results of the renal clearance calculation using the methods described above are reasonably close to each other at 6.4 L/h. The terminal elimination half-life of this drug is between 10 and 20 h. No practical difficulties occurred in the urine collections taken over an adequate period of five to six terminal elimination half-lives. However, for drugs with a prolonged terminal elimination half-life, more than one month of urine collection will cause compliance issues in the clinical study. In this case, the methods stated by Equations 15.2 and 15.4 gain an obvious advantage over the method approaching infinity.

TABLE 15.2 Plasma and Urine Data and Renal Clearance of a Drug Following a Single IV Administration to a Normal Healthy Volunteer

Time Interval (h)	Amount of Unchanged Drug Excreted in Urine (μg)	Urinary Excretion Rate (μg/h)	Mid Plasma Concentration Between Time Interval (ng/mL)	AUC in Plasma Within Time Interval (ng h/mL)	Renal Clearance[a] (L/h)
0–12	5869	489	75.2	929	6.32
12–24	1866	156	24.4	299	6.37
24–48	1540	64.2	12.2	203	7.58
48–72	499	20.8	6.87	78.2	6.38
72–96	223	9.30	3.60	41.1	5.44
>96	202	—	—	10.3	—
0–∞	9997	—	—	1561	6.40

[a]Calculated by equation $CL_R = \frac{A_{e(t_2-t_1)}}{AUC_{(t_2-t_1)}}$.

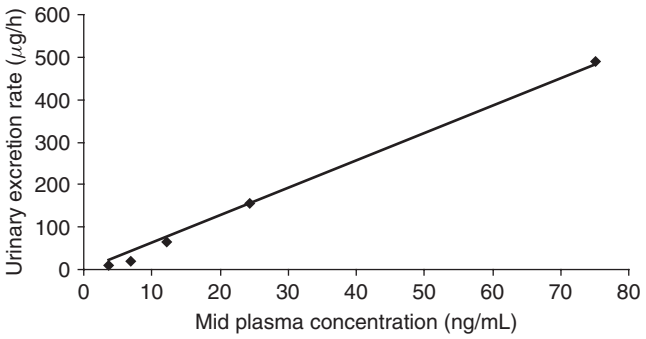

Figure 15.3 Relationship between the urinary excretion rate of a drug and the plasma concentration of the drug at the midpoints of each sample collection interval. The slope of the regression line is equal to the average renal clearance of the drug over 96-h sample collection period. The intercept of the regression line was forced to zero during regression analysis. Renal clearance = 6.43 L/h; $R^2 = 0.9939$.

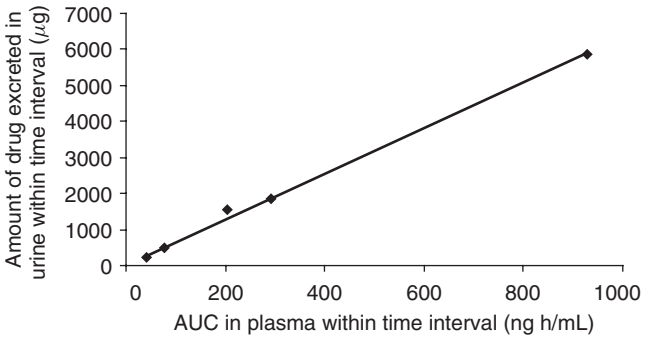

Figure 15.4 Relationship between the amount of unchanged drug excreted in urine and AUC of drug in plasma within each sample collection interval. The slope of the regression line is equal to the average renal clearance of the drug over 96-h sample collection period. The intercept of the regression line was forced to zero during regression analysis. Renal clearance = 6.37 L/h; $R^2 = 0.9969$.

15.4.2 Fraction of Unchanged Drug Excreted in Urine

The fraction of the amount of drug entering the systemic circulation that is excreted unchanged in urine (f_e) is an important PK parameter that indicates the major pathway of drug elimination through either the excretion of unchanged drug via the kidney or metabolism in the liver followed by the excretion of the metabolite(s) in urine. The value of f_e ranges between 0 and 1.0 depending on the extent to which a drug is renally excreted compared to the overall drug elimination. When the value is low, excretion is a minor pathway of drug elimination, suggesting that the most amount of the drug administered is metabolized. If renal excretion is the major route of elimination, the value of f_e will be higher with an upper limit of 1.0, which means that the renal excretion is the only route of drug elimination. The value of f_e for a particular drug will remain constant independent of the dose of the drug administered via IV injection and is estimated by

$$f_e = \frac{U^\infty}{\text{Dose}} \tag{15.5}$$

where U^∞ is total drug excreted unchanged. If the drug is administered orally, f_e is defined by

$$f_e = \frac{U^\infty}{F \times \text{Dose}} \tag{15.6}$$

where F represents the absolute bioavailability of a drug. In the case of a hypothetical drug with urine and plasma data listed in Table 15.2, the amount of unchanged drug excreted in urine is calculated by multiplying urine drug concentration and the urine volume collected within a time interval, and summing the amount from all intervals, giving the value of 9.997 mg. If the IV dose is 200 mg, the f_e is equal to 0.05. In practice, care should always be taken to ensure collecting urine for at least five elimination half-lives.

In those situations in which total urine collection is impossible, f_e may be estimated by the ratio of renal and total clearances,

$$f_e = \frac{k_{ren}}{\lambda_z} = \frac{CL_R \cdot C}{CL \cdot C} = \frac{CL_R}{CL} \tag{15.7}$$

where k_{ren} is the urinary excretion rate constant, λ_z the first-order elimination rate constant, C the plasma drug concentration, CL_R the renal clearance, and CL the total clearance. The CL_R can be estimated from the urine data described in the previous section, while CL can be determined from the plasma data,

$$CL = \frac{\text{Dose}}{\text{AUC}} \tag{15.8}$$

where AUC is the total area under the plasma concentration–time curve. This calculation of clearance is independent of the shape of the concentration–time profile. For a drug with linear PK, the value of clearance is also independent of dose.

15.5 PHARMACOKINETIC ANALYSIS OF PLASMA DATA WITH COMPARTMENTAL MODEL

The compartmental model approach for analyzing PK data is typically to fit a concentration–time profile with a mono-, bi-, or triexponential equation. Computer fitting concentration–time data obtained from a clinical study, including human ADME study, will provide disposition rate constants, which can be used for estimating more PK parameters such as CL, V, absorption rate constant (k_{01}), and elimination rate constant (k_{10}). Since the number of subjects in human ADME study is limited, the PK data from this type of study are frequently pooled with the data from the other human studies of the drug for determining these PK parameters which can be further used in exposure–response analysis. In this case with a large PK dataset, a population PK approach can be applied to estimate inter- and intrasubject variability in addition to the classic PK parameters. With the variability, the PK of a drug and further the exposure–response correlation, if there is any, can be simulated and predicted for certain dose levels and study outcomes that have not been studied in humans. The most frequently used one-, two-, and three-compartment models are listed in Table 15.3. Since data fitting of concentration–time data is out of the scope of this chapter, readers can reference relevant book [6].

15.5.1 Evaluation of Absorption Kinetics from Plasma Concentration–Time Data

Drug absorption process in the gastrointestinal (GI) tract following oral administration is complex because it involves several processes, including disintegration of a solid dosage form, dissolution of a drug into the gastric fluid, gastric emptying, and the diffusion of a drug molecule across the gut wall. In general, absorption of many drugs after oral administration is assumed to follow a first-order process of which the absorption rate is described by

$$\frac{\mathrm{d}A}{\mathrm{d}t} = FDk_{\mathrm{a}}\mathrm{e}^{-k_{\mathrm{a}}t} \tag{15.9}$$

where A denotes the amount of drug in the body, F the bioavailability, D the dose administered, k_{a} the first-order absorption rate constant, and t the time. This model predicts fast absorption, a peak concentration with an intermediate plateau around it followed by an exponential decrease showed in a hypothetic plasma concentration–time profile (Fig. 15.5).

Under certain circumstances, plasma concentrations following oral administration sharply increase to a peak at which absorption slows and quickly declines with no intermediate plateau, of which this absorption of drugs is better described by zero-order kinetics:

For $t \leq T$,

$$C = \frac{k_0}{k_{10}V_{\mathrm{d}}}\left[1 - \mathrm{e}^{-k_{10}(t-t_0)}\right] \tag{15.10}$$

TABLE 15.3 Basic Pharmacokinetic Compartmental Models

Model	Input	Compartment	Elimination Rate	Equation	Compartmental Scheme
1	IV bolus	1	First order	$C(t) = \frac{D}{V}e^{-k_{10}t}$, $k_{10} = \frac{Cl}{V}$	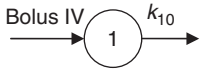
2	First-order extravascular	1	First order	$C(t) = \frac{D \cdot k_{01}}{V(k_{01}-k_{10})}(e^{-k_{10}t} - e^{-k_{01}t})$, $k_{10} = \frac{CL}{V}$	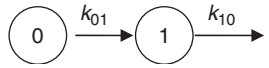
3	IV bolus	2	First order	$C(t) = Ae^{-\alpha t} + Be^{-\beta t}$, $k_{10} = \frac{CL}{V_1}$, $k_{12} = \frac{CL_{D_2}}{V_1}$, $k_{21} = \frac{CL_{D_2}}{V_2}$	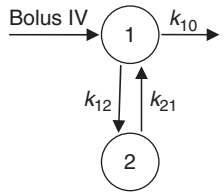
4	First-order extravascular	2	First order	$C(t) = Ae^{-\alpha t} + Be^{-\beta t} + Ce^{-k_{01}t}$, $k_{10} = \frac{CL}{V_1}$, $k_{12} = \frac{CL_{D_2}}{V_1}$, $k_{21} = \frac{CL_{D_2}}{V_2}$	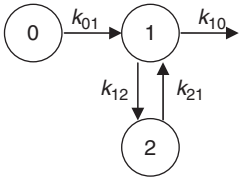
5	IV bolus	3	First order	$C(t) = Ae^{-\alpha t} + Be^{-\beta t} + Ce^{-\gamma t}$	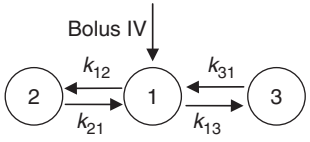

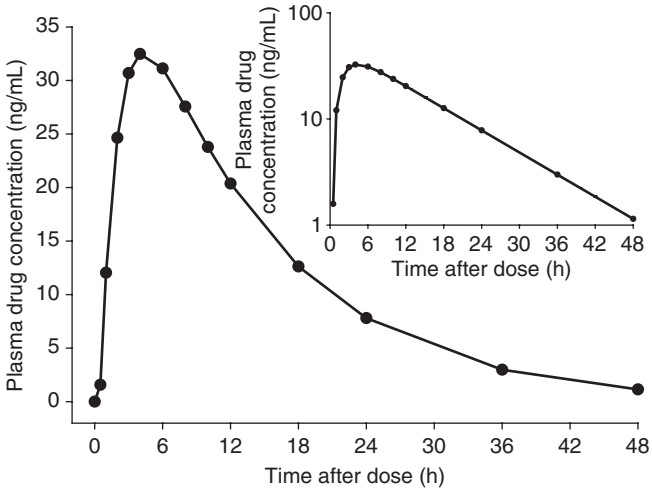

Figure 15.5 Plasma drug concentration–time profile following oral administration of a drug on a linear scale and a semilogarithm scale (inset).

For $t \geq T$,

$$C = \frac{k_0}{k_{10} V_d} \left[1 - e^{-k_{10}(T - t_0)}\right] e^{-k_{10}(t - T)} \tag{15.11}$$

where T represents the time at which absorption stops, k_0 the zero-order absorption rate constant, k_{10} the first-order elimination rate constant, V_d the apparent volume of distribution, and t_0 the lag time.

In some cases, plasma concentrations rise quickly to a high level followed with an exponential decrease. The observed data around the peak are underestimated by the first-order absorption. The combination of zero- and first-order input sometimes can give the best fitting to this type of concentration–time profile [7]. Nevertheless, the zero- and first-order absorption processes are mostly observed for many drugs. The Wagner–Nelson (W–N) method, Loo–Riegelman (L–R), deconvolution, nonlinear regression analysis, and several other methods have been used to estimate zero- and first-order absorption kinetics.

15.5.1.1 Wagner–Nelson (W–N) Method. The one-compartment model is based on the assumption that the dose absorbed is distributed into a single compartment and is eliminated from it by first-order process of metabolism and excretion. This is represented schematically in Table 15.3. Following the principle of mass balance, the amount of unchanged drug reaching the fluid of distribution is the amount of drug absorbed at any time, A_t, by the central compartment, the blood stream. The drug absorbed at a given time is equal to the amount of the drug existing in the central compartment plus the amount metabolized and excreted by all pathways and routes. Wagner and Nelson [8,9] derived several absorption equations on the basis of this mass balance for analyzing single-dose one-compartment absorption kinetic data. Since the rates of metabolism and excretion are often found to be directly proportional to the

blood concentration, they proposed that the amount of the drug eliminated by the time t could be estimated by

$$k V_{\mathrm{d}} \int_{t_0}^{t} C_{\mathrm{p}} \mathrm{d}t \tag{15.12}$$

where V_{d} is the apparent volume of distribution, C_{p} the plasma concentration of drug at the time when drug is absorbed, and k the first-order rate constant for the elimination of the drug from the body and is equal to the sum of the individual rates of metabolism and excretion. Therefore, integration of the differential mass balance equation over the time range of t_0 and t_∞ results in what has been called *W–N absorption equation*:

$$\left(\frac{A}{V_{\mathrm{d}}}\right)_t = C_{\mathrm{p}} + k \int_{t_0}^{t} C_{\mathrm{p}} \mathrm{d}t \tag{15.13}$$

With Equation 15.13, the amount of the drug absorbed at time t expressed in a concentration unit can be evaluated as being the sum of drug concentration in the systemic circulation and the amount eliminated in a concentration unit. When the time approaches to infinity, the amount of the drug absorbed will asymptotically reach the total amount of the drug absorbed. Since the apparent volume of distribution may not be known without IV PK data, often, Equation 15.13 is represented as the fraction of bioavailable drug absorbed, $(F_{\mathrm{ab}})_t$, at time t:

$$(F_{\mathrm{ab}})_t = \frac{C_{\mathrm{p}} + k \int_{t_0}^{t} C_{\mathrm{p}} \mathrm{d}t}{k \int_{t_0}^{\infty} C_{\mathrm{p}} \mathrm{d}t} = \frac{C_{\mathrm{p}} + k \cdot \mathrm{AUC}_{0-t}}{k \cdot \mathrm{AUC}_{\infty}} \tag{15.14}$$

To illustrate the procedure for calculating the fraction of bioavailable drug absorbed, a set of concentration–time data following oral administration of a 200-mg dose of drug is listed in Table 15.4 and displayed in Fig. 15.5. The partial AUC_{0-t} value to each time point is calculated by noncompartmental method following the trapezoidal rule. The k value is estimated from the terminal phase of concentration–time profile with a terminal half-life of 8.65 h. As a result of this terminal half-life, the k value is estimated to be 0.0801/h. The product of $k{\cdot}\mathrm{AUC}_{0-t}$ is then calculated and added to the plasma concentration at time t to yield $(A/V_{\mathrm{d}})_t$. The $\mathrm{AUC}_{0-\infty}$ is calculated by the following equation:

$$\mathrm{AUC}_{0-\infty} = \mathrm{AUC}_{\mathrm{last}} + \frac{C_{\mathrm{last}}}{k} \tag{15.15}$$

where C_{last} and $\mathrm{AUC}_{\mathrm{last}}$ are the concentration of drug at the last PK sampling point and the AUC value from time 0 to the last time point, respectively. With known k and $\mathrm{AUC}_{0-\infty}$ values, the product of $k{\cdot}\mathrm{AUC}_{0-\infty}$ is obtained. Finally, the fraction of bioavailable drug absorbed is calculated by Equation 15.14 and is presented in Fig. 15.6.

TABLE 15.4 Calculation of Cumulative Fraction of Drug Absorbed Using W–N Method

Time (h)	C_p (ng/mL)	AUC_{0-t} (ng h/mL)	$k \cdot AUC_{0-t}$ (ng/mL)	$C_p + k \cdot AUC_{0-t}$ (ng/mL)	$(F_{ab})_t$
0	0	0	0	0	0
0.5	1.58	0.396	0.147	1.73	0.0357
1	12.0	3.80	1.41	13.4	0.274
2	24.7	22.1	8.21	32.9	0.585
3	30.7	49.8	18.5	49.2	0.768
4	32.5	81.4	30.2	62.6	0.864
6	31.1	145	53.7	84.9	0.947
8	27.6	204	75.5	103	0.972
10	23.8	255	94.5	118	0.980
12	20.4	299	111	131	0.982
18	12.6	398	148	160	0.987
24	7.81	460	170	178	0.989
36	2.99	524	194	197	0.997
48	1.14	549	203	205	1.000

$k = 0.0801$/h.

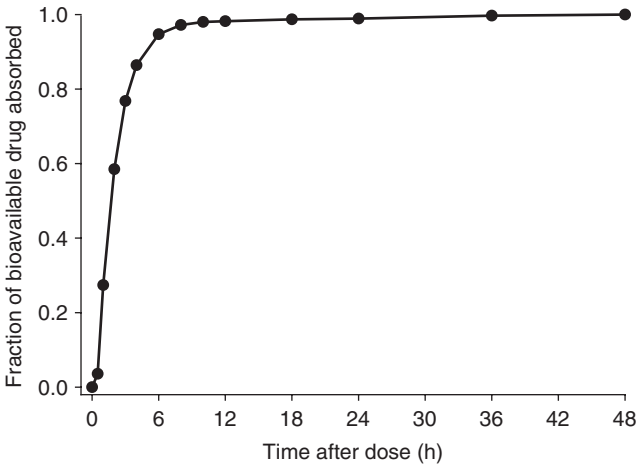

Figure 15.6 Fraction of bioavailable drug absorbed as function of time after dose.

To utilize W–N method to analyze absorption behavior of a drug, it is not necessary to have IV data available for this drug. The issue with oral PK data alone is inaccuracy in estimating elimination rate constant, k. This is because in some cases, absorption following oral administration is taking place at the same time as drug clearance, tri-exponential drug distribution into the peripheral tissue compartment, or absorption continues well beyond the peak in the concentration–time profile. The mixed distribution and elimination phase frequently shows a longer terminal half-life compared to that following an IV bolus infusion in which the drug is instantly distributed into the blood stream. Therefore, accurate estimate of elimination rate constant has to rely on the PK data following IV bolus infusion.

15.5.1.2 Loo–Riegelman (L–R) Method. When a drug has been administered intravenously first, then extravascularly second, disposition of the drug shows bi- or triexponential. Loo and Riegelman [10] have proposed a mathematically and physiologically more acceptable method to conceive the body to be a two-compartment open system. The scheme and equation for this type of model are presented in Table 15.3.

It is convenient to express all the drug amounts as concentration terms by dividing by V_p, whereupon they become the concentrations in central (C_p) and tissue (C_t) compartments as well as the concentrations of metabolized and excreted drug (C_{me}). Therefore, C_{me} up to time t becomes

$$(C_{me})_{in} = k_{10} V_d \int_{t_0}^{t} C_p dt \tag{15.16}$$

Integration of the differential equation between the time limits of 0 and t obtains

$$\left(\frac{A}{V_p}\right)_{in} = (C_p)_{in} + k_{10} V_d \int_{t_0}^{t} C_p dt + (C_t)_{in} \tag{15.17}$$

This is a form of modified W–N equation for the two-compartment model. Taking the similar approach to W–N equation, the fraction of bioavailable drug absorbed, $(F_{ab})_t$, through a first-order process and eliminated through a second-order process at time t becomes

$$(F_{ab})_t = \frac{C_p + C_t + k_{10} \int_{t_0}^{t} C_p dt}{k_{10} \int_{t_0}^{\infty} C_p dt} = \frac{C_p + C_t + k_{10} \cdot AUC_{0-t}}{k_{10} \cdot AUC_{\infty}} \tag{15.18}$$

The concentration of drug in the central compartment C_p can be determined with plasma samples using a validated bioanalytical method. However, the concentration of the drug in peripheral (tissue) has to be estimated from the distribution rate constants between central and peripheral compartments with an assumption of a linear function on drug concentrations in the central compartment between two mostly closed time points. After approximation, the differential equation of

$$\frac{dC_t}{dt} = -k_{21} C_t + k_{12} C_p \tag{15.19}$$

becomes integratable by Laplace transforms and the second term of the equation can be simplified by a two-term Taylor approximation. Therefore, the concentration of drug in tissue compartment can be estimated by the following equation:

$$(C_t)_{t_n} = \frac{k_{12} \cdot \Delta C_p \cdot \Delta t}{2} + \frac{k_{12}}{k_{21}} (C_p)_{t_{n-1}} \cdot \left(1 - e^{-k_{21} \cdot \Delta t}\right) + (C_t)_{t_{n-1}} \cdot e^{-k_{21} \cdot \Delta t} \tag{15.20}$$

where t_n and t_{n-1} are the sample times for samples n and $n-1$, respectively, $(C_p)_{t_{n-1}}$ is the concentration of drug at the central compartment for samples $n-1$ and $(C_t)_{t_n}$

and $(C_t)_{t_{n-1}}$ are the concentrations of drug at the tissue compartment for samples n and $n-1$, respectively.

15.5.1.3 Gamma Model of Absorption. Absorption of some drugs that show flat and delayed absorption profiles with a correlation between delay and peak width may not obey the zero- or first-order absorption model described above. A gamma model that describes an asymmetric S-shaped curve with an early flat phase was developed by Debord *et al*. [11] to predict oral cyclosporin PK profile:

$$\frac{dA}{dt} = FD \cdot f(t) \tag{15.21}$$

$$f(t) = \frac{b^a}{\Gamma(a)} t^{a-1} e^{-bt} \tag{15.22}$$

where dA/dt denotes the absorption rate at time t, a the number of sequential compartments connected by an identical input rate constant b (Fig. 15.7), and Γ the gamma function defined by

$$\Gamma(a) = \int_0^\infty x^{a-1} e^{-x} dx \tag{15.23}$$

The convolution of the absorption rate at time t dA/dt with the impulse response of a two-compartment model gives the equation for drug blood concentration at time t:

$$I(t) = A_1 e^{-\lambda_1(t)} + A_2 e^{-\lambda_2(t)} \tag{15.24}$$

where $I(t)$ is the concentration at time t following, A_1 and A_2 are the disposition coefficients, and λ_1 and λ_2 are the disposition rate constants.

Figure 15.8 shows an example in which a good fit is obtained with the gamma function, whereas a poor fit is obtained with a classic exponential model with lag time.

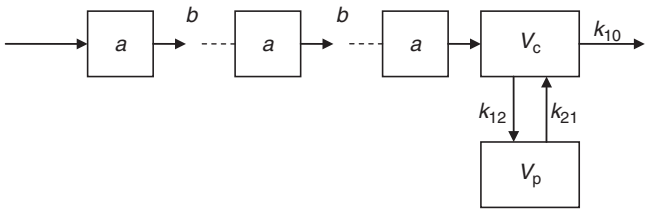

Figure 15.7 Gamma distribution model as a sequence of identical compartments (a) connected by an equal rate constant (b) with an input toward a central compartment followed with a distribution process between the central compartment and peripheral compartment and with a linear elimination process from the central compartment.

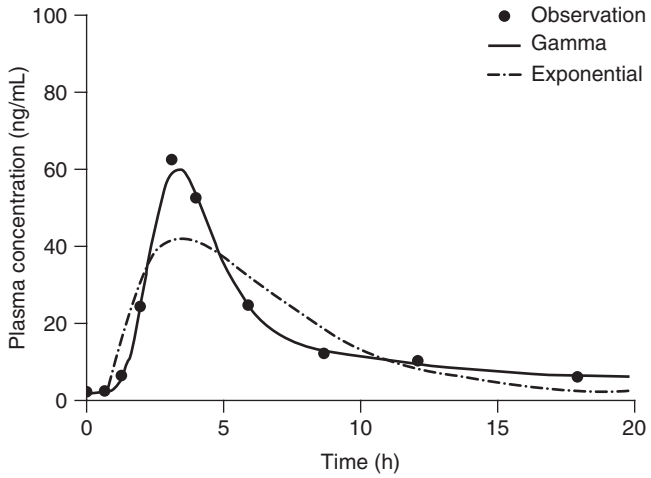

Figure 15.8 Comparison of gamma absorption and a classic exponential with lag-time models.

15.5.1.4 Discontinuous Absorption Model. Delayed gastric emptying of a portion of an orally administered dose can cause double peaks or irregular shape in the absorption and early distribution phases of concentration–time profiles. The factors other than delayed gastric emptying, such as enterohepatic recirculation, storage, and subsequent release of drug from a postabsorptive depot site, may also be responsible for the double peaks. However, the second peak under these circumstances may occur in the distribution phase of the concentration–time profile. A discontinuous absorption model has been developed to describe a drug absorption process along the gastric tract with distinct double peaks in the early phase of concentration–time profile.

The discontinuous absorption model [12] assumes that two absorption sites exist separately in the GI tract. The entire dose is loaded into the first gut compartment with a zero-order input and the drug in the first gut compartment transfers to the second gut compartment, which is the first absorption site. Absorption to the central compartment does not take place in intervening regions between the two absorption sites. When the entire drug moves to the second absorption site, absorption ceases. The amount of drug entering the first absorption site is dependent on the dose and the rate of drug entering the site (k_1). The transition rate (k_t) into the second absorption site is dependent on the efficiency of the first absorption site, the distance between the two absorption sites, and the transition rate in the nonabsorption regions of the gut. All rate constants in the discontinuous model, including transition rate constants in the gut (k_1 and k_t), absorption rate constants (k_{a1} and k_{a2}), and elimination rate constant (k_{10}) are assumed to be first-order rate constants (Fig. 15.9). The equation to describe the fraction of drug in each compartment is solved using Laplace transforms. The drug in central compartment is given by

$$L(A_C) = \frac{[k_{a1} \cdot L(A_2) + k_{a2} \cdot L(A_N)]\,(s + k_{21})}{[(s + k_{21})(s + k_{10} + k_{12})] - k_{21} \cdot k_{12}} \tag{15.25}$$

where $L(A_C)$, $L(A_2)$, and $L(A_N)$ are the Laplace transforms for drug flux in the central compartment and the two absorption compartments, respectively, and s is the Laplace operator.

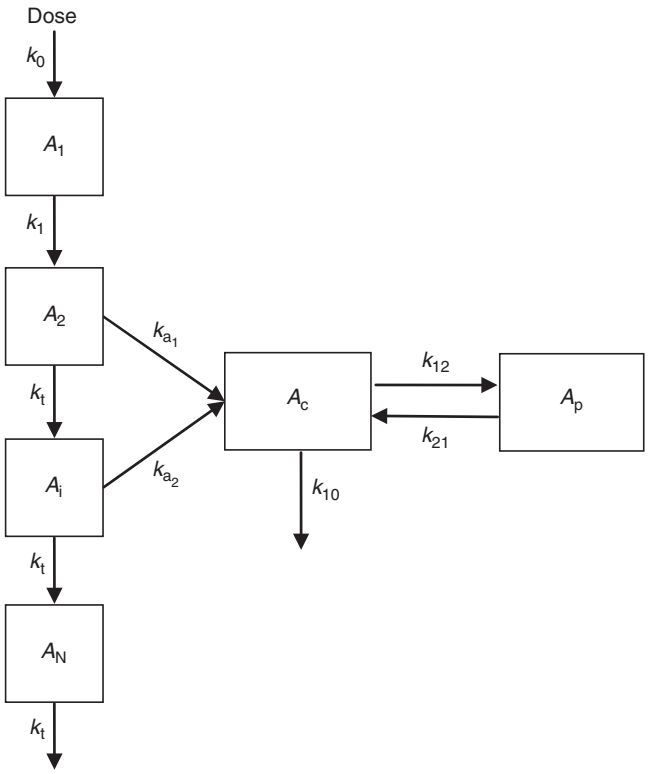

Figure 15.9 Discontinuous oral absorption pharmacokinetic model.

The ratio of the absorption rate constant at one specific site to the sum of all rate constants in this absorption compartment represents the theoretical fraction of drug absorbed at this site. For example, the fractions of drug absorbed at the first and second absorption sites F_1 and F_2, respectively, are as the follows [12]:

$$F_1 = \frac{k_{\mathrm{a1}}}{k_t + k_{\mathrm{a1}}} \tag{15.26}$$

$$F_2 = \frac{(1 - F_1)k_{\mathrm{a2}}}{k_t + k_{\mathrm{a2}}} \tag{15.27}$$

The simulated effect of changes in the number of gut compartments (N), transition rate constant (k_t), and absorption rate constants (k_{a1} and k_{a2}) are plotted in Fig. 15.10. As N increases, the time to reach the second peak is delayed and the concentration in the second compartment decreases. Where the k_t value becomes large, the second peak occurs shortly after the first peak and the fraction of drug absorbed from both the absorption sites is also reduced. The values of k_{a1} and k_{a2} determine the height of these two peaks. The high absorption rate produces a high peak associated with this absorption process.

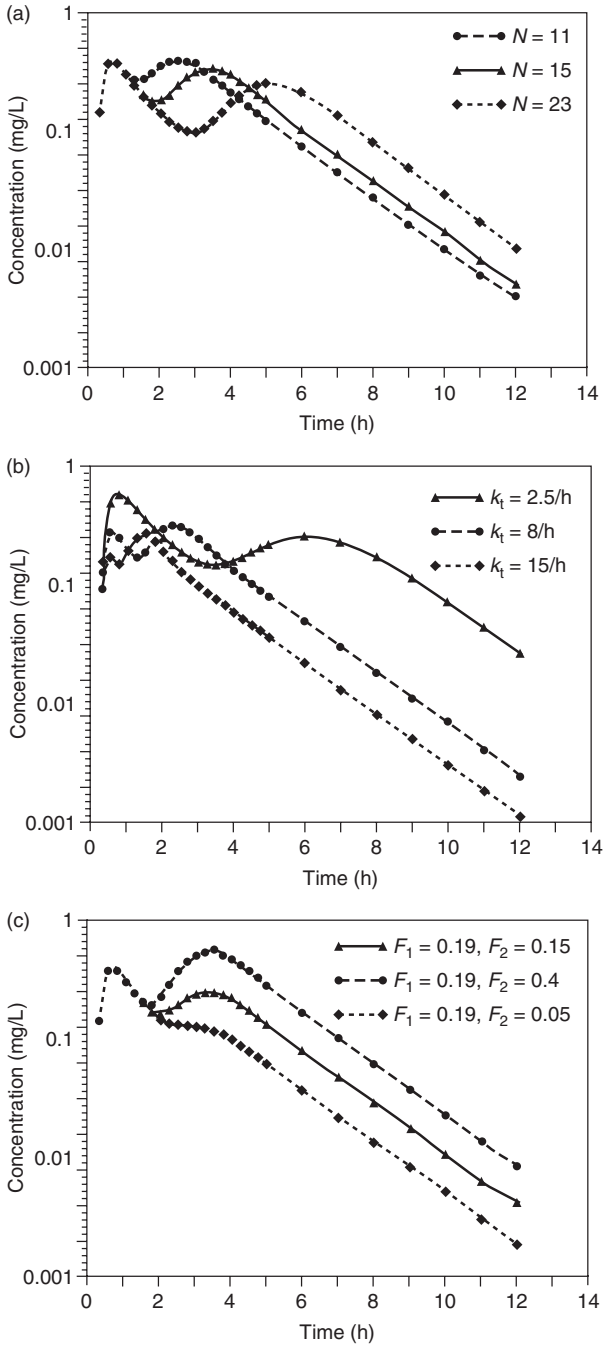

Figure 15.10 Simulated concentration–time profile following oral administration of a hypothetic drug based on a discontinuous gastrointestinal absorption model [12]. (a) Influence of the total number of gut compartments (N). (b) Influence of drug transition rate (k_t) between absorption sites. (c) Influence of the fraction of drug absorbed at the first and second absorption sites.

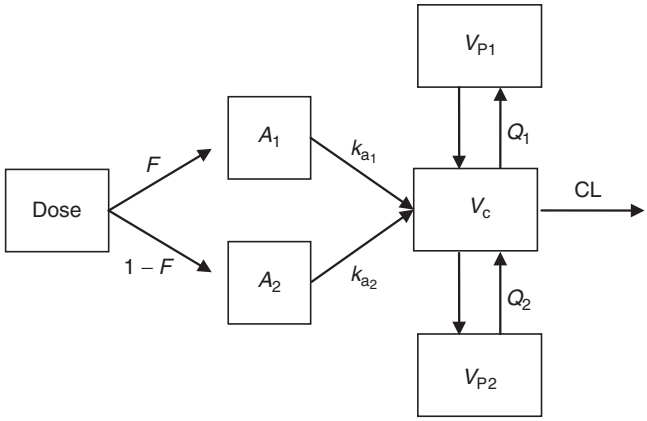

Figure 15.11 Parallel oral absorption pharmacokinetic model.

15.5.1.5 Parallel Absorption Model. When two or more concentration peaks are not distinct in a concentration–time profile, a parallel absorption model can be used to fit these PK data. Figure 15.11 shows the scheme of a dual absorption pathway model with two different first-order absorption rate constants (k_{a1} and k_{a2}) and two different lag times. The drug administered enters two different gut compartments with the different fractions of dose, F and 1 – F, divided into the rapidly and delayed absorbed subdoses. The drug in the gut compartments is then absorbed into the central compartment in which the drug is either exchanged between the central compartment and two different peripheral compartments or eliminated from the central compartment. A two-compartment model may fit the two-peak concentration–time profiles with less precise parameter estimates due to underparameterization. A three-compartment model is in general superior to the two-compartment model in fitting the slowly declining terminal phase of concentration–time data. The three-compartment model with two parallel absorption processes schematically depicted in Fig. 15.11 was used to describe the PK of piperaquine administered with concomitant CV8 [13].

In summary, a delayed peak or multiple peaks that are not so uncommon atypical absorption phenomena after oral drug administration may occur due to the delayed release of drug from its dosage form, cyclical gastric emptying, or influences by intake of food. The clinical implication of these atypical absorption processes should be considered. The compounds with a delayed peak may not be suitable as a medication to treat disorders where rapid t_{max} and high C_{max} are important in clinical efficacy. Compounds with multiple peaks may cause some safety issues, especially for those drugs with a narrow therapeutic index.

15.5.2 Evaluation of Distribution Kinetics from Plasma Concentration–Time Data

Drug distribution in the body can be influenced by different processes, including enterohepatic recirculation, various transport mechanisms, and drug binding to tissue and proteins as well as metabolism. In some cases, the distribution curve of drugs is significantly affected by these processes so that the normal pattern of smooth decreases

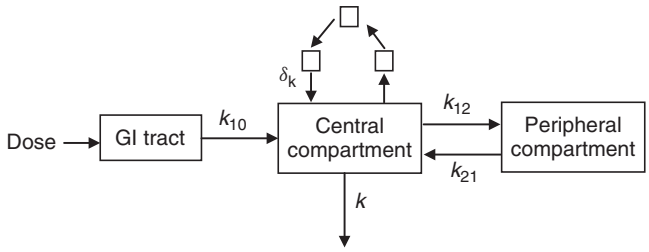

Figure 15.12 The enterohepatic recirculation model consists of a central compartment, a peripheral compartment, and the circulation chain that includes three compartments each of fixed volume.

in plasma concentrations does not exist, resulting in double peaks or multiple peaks when enterohepatic recirculation is the primary process of drug distribution. The typical compartmental models are no longer applied to this type of distribution. More complex PK models are needed to predict drug concentration in circulation that will provide useful information regarding optimal dosing and potential exposure–response correlation.

15.5.2.1 Modeling Enterohepatic Recirculation. The drugs that experience enterohepatic recirculation will show at least two peaks in the plasma concentration–time profile. After oral administration, a dose D reaches the absorption compartment (GI tract). A fraction of the dose is absorbed by a first-order process reaching the central compartment. The drug absorbed is distributed from the central compartment 1 to the peripheral compartment 2 and is eliminated from the central compartment 1 by first-order process if the concentration–time profile can be described by a two-compartment model. Some fraction of the dose absorbed in the central compartment will be added back to the systemic circulation at time τk as a secondary input into the systemic circulation (Fig. 15.12). A two-compartment PK model incorporated with enterohepatic recirculation is as follows [14]:

$$C_j(t) = C_{\text{pred},j}(t) + \delta_1 \cdot C_{\text{pred},j}(t - \tau_1) + \delta_2 \cdot C_{\text{pred},j}(t - \tau_2) + \cdots + \delta_n \cdot C_{\text{pred},j}(t - \tau_n) + \varepsilon_j(t) \tag{15.28}$$

where $C_j(t)$ and $C_{\text{pred, j}}(t)$ are the measured and predicted concentrations for the jth subject at time t, respectively, and δ fraction of drug due to enterohepatic recirculation is added back to the systemic circulation at time τk where k is the number of events. An assumption is held for this model that a drug accumulates in a certain compartment or compartments and retains there for some time, then it returns into the circulation system, which eventually results in the second peak of $C_j(t)$. The phenomenon of the second peak in the distribution phase has been observed in species that have a gall bladder, when hepatic recirculation of drug occurs as periodical release of bile into the duodenum with subsequent reabsorption of drug into the circulation system. Random effects, ε, were supplemented to the fraction that will be added back to the circulation and the gall bladder emptying time to account for variability. The model using the nonlinear mixed-effects function provided a good fitting of most individual

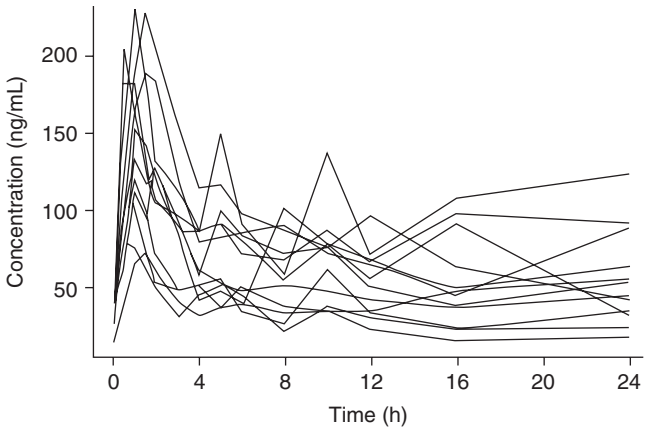

Figure 15.13 Plasma ezetimibe concentration–time profiles with enterohepatic recirculation after multiple-dose administration of ezetimibe [14].

plasma concentration–time profiles for ezetimibe following dose administration [13] and is presented in Fig. 15.13.

15.5.2.2 Modeling Blood–Brain Barrier Transport. Compartmental PK analysis has been applied to characterize the drug concentration–time course in systemic circulation and the brain extracellular fluid (bECF) simultaneously with the advantage over traditional noncompartmental methods where the compartmental analysis quantifies the rate of blood–brain barrier (BBB) transport independent of differences in systemic exposure. This allows comparison of *in vivo* with *in vitro* PK parameters and comparison between compounds that have different systemic PK properties. Furthermore, modeling the bidirectional distribution to and from the brain may reveal the process that determines the time course of drug effect to help design preclinical and clinical studies and interpret pharmacological data from these studies.

A two-compartment model in systemic circulation connected to a one-compartment brain model that is separated by a BBB was proposed to fit unbound plasma and bECF escitalopram concentrations simultaneously in rats [15]. This structure of the model is depicted in Fig. 15.14. Using intracerebral microdialysis, quantitative information about the free drug concentrations at the extracellular target site in the discrete areas of the rodent brain can be obtained. The general differential equations associated with this model are as follows:

$$\frac{dC_1}{dt} = \frac{\text{input}}{V_1} + \frac{k_{21}C_2V_2}{V_1} + \frac{k_{out}C_{bECF}V_{bECF}}{V_1} - (k_{10} + k_{12} + k_{in})C_1 \quad (15.29)$$

$$\frac{dC_2}{dt} = \frac{k_{12}C_1V_1}{V_2} - k_{21}C_2 \quad (15.30)$$

$$\frac{dC_{bECF}}{dt} = \frac{k_{in}C_1V_1}{V_{bECF}} - k_{out}C_{bECF} \quad (15.31)$$

where C_1 and C_2 denote the drug concentrations in the central and peripheral plasma compartments and C_{bECF} is the extracellular concentration in the brain. Input represents

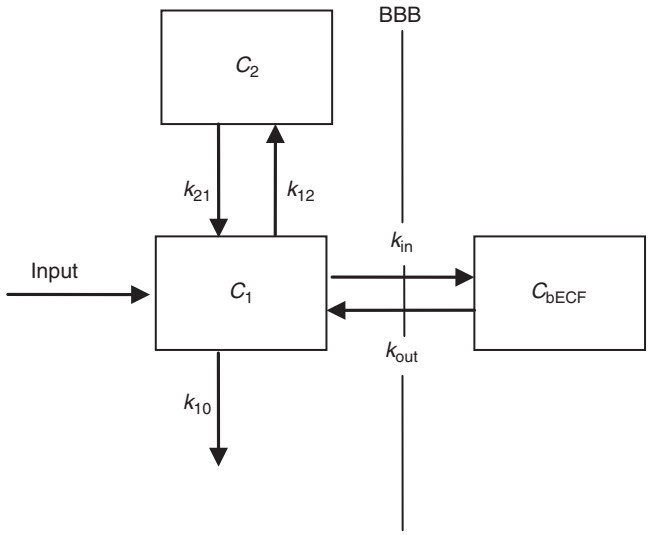

Figure 15.14 Compartmental model of drug transport between plasma and brain extracellular fluid following intravenous injection.

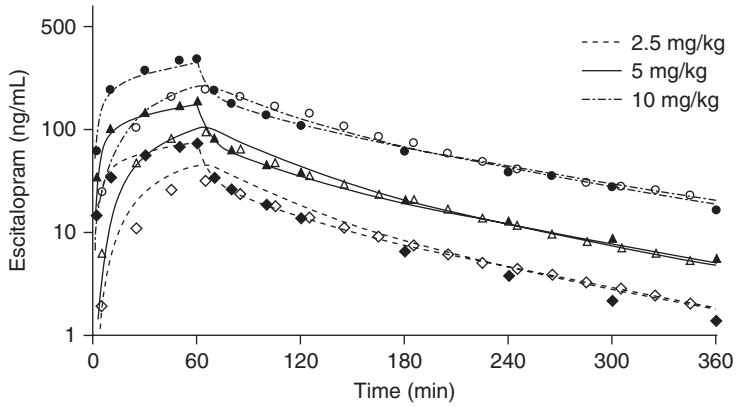

Figure 15.15 Observed (mean) and model-predicted unbound escitalopram concentration–time profiles in plasma (filled symbols) and brain extracellular fluid (open symbols) following intravenous infusion of 2.5-, 5-, and 10-mg/kg escitalopram [15].

the administered dose via IV injection. The k and V signify the rate constant and volume of distribution as detailed in Fig. 15.14. This model was successfully fit to the unbound escitalopram concentration–time profiles in plasma and bECF obtained in an experiment in rats (Fig. 15.15).

Solving the compartmental model provides both the extent and rate of drug transport to brain. The extent of equilibrium across the BBB is influenced by the involvement of active membrane transport mechanisms located at the endothelial cells in the BBB, whereas the rate of drug transport across the BBB is related to physiochemical properties of drug. These PK characteristics will affect the degree, onset, and duration of the

centrally medicated effect. A final BBB model is established on the basis of an iterative analysis of the experimental data using a variety of different models. Both systemic and brain models vary from one- to multiple-compartments and from a linear model to a nonlinear model such as Michaelis–Menten (M–M) model. The goodness-of-fit is employed to select the best model for fitting the experimental data.

15.5.3 Evaluation of Metabolism Kinetics from Plasma Concentration–Time Data

15.5.3.1 Compartmental Analysis of Metabolites. The data analysis of metabolite plasma concentration–time data using a compartmental approach is similar to the analysis for the disposition of parent drug in systemic circulation. Compartmental modeling to include metabolites is more complicated than that for parent drug alone because this type of model need not only characterize parent drug but also requires a link between parent and metabolite as well as possible involvement of nonlinear kinetics. For modeling with parent drug only, the methodical, conceptual, and computational uniformity in modeling various linear biological systems is the dominant characteristic of the linear system approach technology. However, saturation of the metabolic reaction results in nonlinear kinetics.

Figure 15.16 represents an integrated open two-compartment model for a parent drug and an open one-compartment model for the metabolite of the parent drug. Assuming

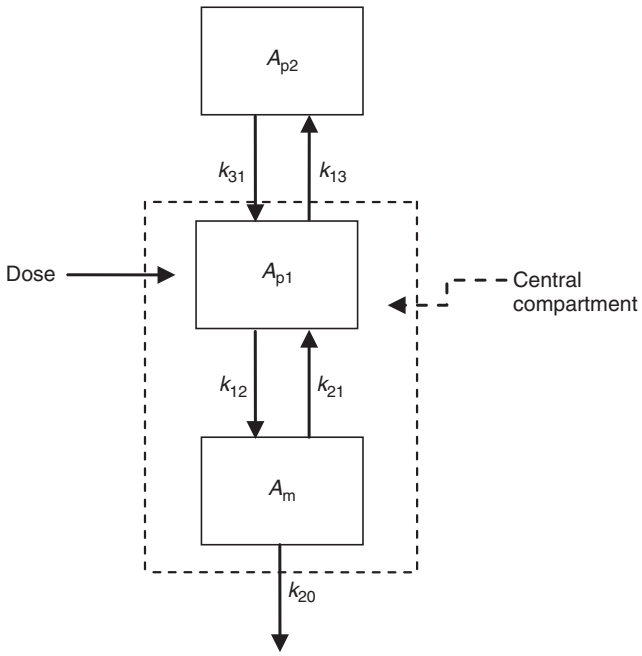

Figure 15.16 A compartment model in which a parent drug is characterized by a two-compartment model and a metabolite is assessed by a one-compartment model. A_{p1} and A_{p2} are the amount of a parent drug in the central compartment and peripheral compartment, respectively. A_m is the amount of the metabolite in the central compartment of the metabolite.

both input and disposition functions are linear, the model can be solved by the Laplace transform with a general fraction theorem. The amount of parent drug (A_{p1}) in the central compartment may be written [16]:

$$A_{P1} = \frac{(k_{20}k_{21} - \alpha)(k_{31} - \alpha)D}{(\beta - \alpha)(\gamma - \alpha)} e^{-\alpha t} + \frac{(k_{20}k_{21} - \beta)(k_{31} - \beta)D}{(\alpha - \beta)(\gamma - \beta)} e^{-\beta t} + \frac{(k_{20}k_{21} - \gamma)(k_{31} - \gamma)D}{(\alpha - \gamma)(\beta - \gamma)} e^{-\gamma t} \quad (15.32)$$

where α, β, and γ are coefficients of the powers, $k_{i,j}$ is the first-order rate constant describing transfer from compartment i to compartment j, t is the time postdose, and D is the dose. The amount of metabolite (A_m) in the central compartment can be expressed as follows:

$$A_m = \frac{k^\circ(k_{20}k_{21} - \alpha)(k_{31} - \alpha)(1 - e^{\alpha b})}{-\alpha(\beta - \alpha)(\gamma - \alpha)} e^{-\alpha t} + \frac{k^\circ(k_{20}k_{21} - \beta)(k_{31} - \beta)(1 - e^{\beta b})}{-\beta(\alpha - \beta)(\gamma - \beta)} e^{-\beta t} + \frac{k^\circ(k_{20}k_{21} - \gamma)(k_{31} - \gamma)(1 - e^{\gamma b})}{-\gamma(\alpha - \gamma)(\beta - \gamma)} e^{-\gamma t} \quad (15.33)$$

where k° is zero-order infusion rate in units of amount per time and b the time when infusion ends. The above equation applies when the infusion begins at a time zero. For continuous infusion, b is equal to t and varies with t. When infusion ends, b becomes constant corresponding to the duration of infusion. In the above model, drug metabolism is described by linear models assuming the concentration of the involved enzyme is high with respect to the drug concentration. However, in many cases, drug concentration in systemic circulation is much higher than enzyme concentration at a metabolic reaction site. This leads to saturation of drug at the enzyme reaction sites, resulting in zero-order kinetics. While drug concentration is at intermediate level, the M–M equation, a nonlinear model, appropriately describes drug disposition, as discussed in Section 15.5.4.3.

A parent–metabolite model was developed to assess the disposition of artesunate (AS) and its active metabolite dihydroartemisinin (DHA) in healthy subjects receiving single or multiple dosing of AS orally [17]. The structure of the model is depictured in Fig. 15.17, which consists of a one-compartment model with first-order absorption and first-order elimination describing the AS concentration–time profile and a two-compartment model with one central and one peripheral compartment for DHA. With this model, the data for both AS and DHA were analyzed simultaneously with a population PK approach nonlinear mixed effects modelling (NONMEM). The model was stable and was able to predict AS and DHA concentration–time data following single and repeat dosing of oral AS equally well.

15.5.3.2 Compartmental Analysis of Drug–Drug Interaction. Concomitantly administered drugs often cause one-direction or mutual impact by increasing or decreasing the systemic exposure of drugs. As a result of the interaction, the probability of causing adverse events may be higher due to increased drug concentration in blood or efficacy of the affected drug may decrease with lowered plasma drug concentration. In human drug–drug interaction (DDI) studies, both parent drug and metabolite

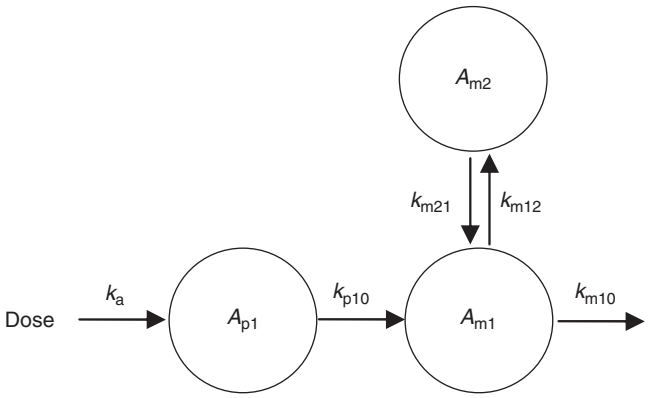

Figure 15.17 Scheme of a parent–metabolite model following oral administration of a parent drug. A_{p1} is the amount of a parent drug in the central compartment. A_{m1} and A_{m2} are the amount of the metabolite in the central and peripheral compartments of the metabolite, respectively. k_a is the absorption constant. k_{p10} and k_{m10} are the elimination rate constants for the parent and the metabolite, respectively. k_{m12} and k_{m21} are the distribution rate constants for the metabolite.

plasma concentration–time profiles may be assessed simultaneously. Evaluation of the PK parameters of the parent drug and its metabolite(s) can provide information on DDI. In an example presented below, the mutual effect of two anticancer agents thiotepa (TT) and cyclophosphamide (CP) is evaluated by a compartment PK model [18].

The prodrug (CP) is metabolized and bioactivated by CYP isoenzymes to form 4-hydroxycyclophosphamide (HCP) that exerts cytotoxicity in the target cells [18]. The resulting metabolite, HCP, is further metabolized to phosphoramide mustard (PM). These metabolites induce CYP enzymes through a process called *autoinduction*. CP is also metabolized through a noninducible side-chain oxidation, resulting in the formation of 2-dechloroethylcyclophosphamide. On the other hand, TT is metabolized to its main metabolite tepa (T) mediated by CYP2B and 2 C. T has pharmacological properties similar to parent TT. When CP is coadministered with TT, the latter inhibits the CYP enzymes responsible for the biotransformation of CP to HCP, resulting in a decrease in HCP concentrations. Meanwhile, CP increases the rate of metabolism of TT to T. These processes represent a mutual DDI between CP and TT and make PK modeling more complicated.

The compartment PK DDI model is schematically pictured in Fig. 15.18. In this model, 2 two-compartment models with first-order elimination from the central compartments of TT and T, respectively, are used to characterize the concentration–time profiles of both TT and T. TT as a perpetrator inhibits CYP enzymes so that bioactivation from CP to HCP is reduced [18]. A two-compartment model and a one-compartment model describe the PK profiles of CP and HCP, respectively. Elimination from the central compartment of CP consists of two pathways, a noninducible route and an inducible route of which the latter leads to the formation of HCP. Both models to describe the time course of CP and TT include two different hypothetical enzyme compartments. In the first hypothetical enzyme compartment, the time course of CP autoinduction is modeled. Biotransformation from CP to HCP is directly proportional to the amount of enzyme in this compartment, whereas TT produces inhibition to

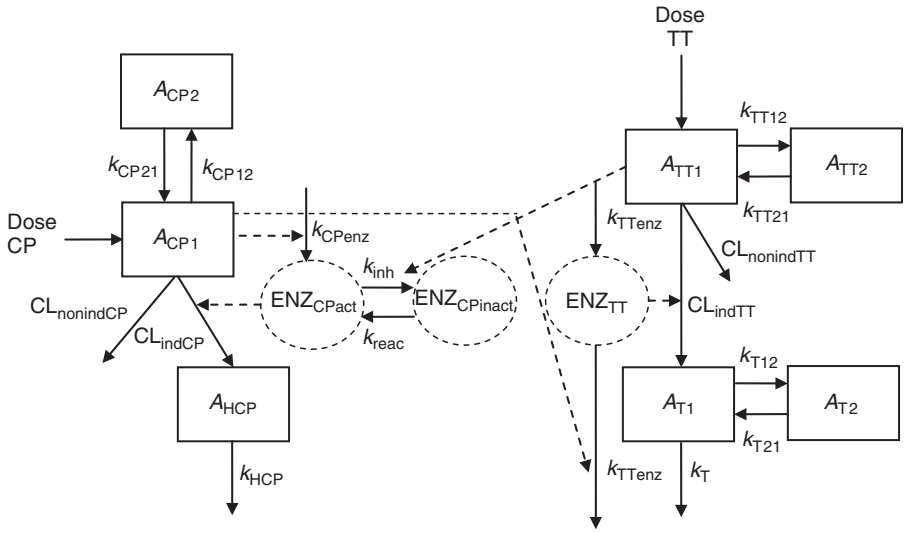

Figure 15.18 Integrated two-compartment models for mutual drug–drug interaction between cyclophosphamide and thiotepa [18].

the metabolism. In the second hypothetical enzyme compartment, an enzyme turnover model, including a zero-order enzyme formation model and a first-order enzyme elimination model, appropriately describes TT and T data. Enzyme elimination is inhibited in the presence of CP with an E_{max} model. When CP infusion starts, the amount of enzyme in the second hypothetical enzyme compartment begins increasing until a maximum amount of enzyme is reached as a result of decreased enzyme elimination by CP. The differential equations describing the mass transport of the different compartments of the model are as follows [18].

Differential equations for the central compartments:

$$\frac{dA_{CP1}}{dt} = R_{CP} - \frac{CL_{nonindCP} A_{CP1}}{V_{CP}} - \frac{CL_{ind} A_{CP1} A_{ENZCP}}{V_{CP}} - k_{CP12} A_{CP1} + k_{CP21} A_{CP2} \tag{15.34}$$

$$\frac{dA_{TT1}}{dt} = R_{TT} - \frac{CL_{nonindTT} A_{TT1}}{V_{TT}} - \frac{CL_{indTT} A_{TT1} A_{ENZTT}}{V_{TT}} - k_{TT12} A_{TT1} + k_{TT21} A_{TT2} \tag{15.35}$$

$$\frac{dA_{HCP}}{dt} = \frac{CL_{indCP} A_{CP1} A_{ENZCP}}{V_{CP}} - k_{HCP} A_{HCP} \tag{15.36}$$

$$\frac{dA_{T1}}{dt} = \frac{CL_{indTT} A_{TT1} A_{ENZTT}}{V_{TT}} - k_{T12} A_{T1} + k_{T21} A_{T2} - k_T A_{T1} \tag{15.37}$$

Differential equations for the peripheral compartments:

$$\frac{dA_{CP2}}{dt} = k_{CP12} A_{CP1} - k_{CP21} A_{CP2} \tag{15.38}$$

$$\frac{dA_{TT2}}{dt} = k_{TT12}A_{TT1} - k_{TT21}A_{TT2} \tag{15.39}$$

$$\frac{dA_{T2}}{dt} = k_{T12}A_{T1} - k_{T21}A_{T2} \tag{15.40}$$

Differential equations for the enzyme compartments:

$$\frac{dA_{ENZCPact}}{dt} = \frac{k_{CPenz}C_{CP1}}{IC_{50} + C_{CP1}} - k_{inh}A_{TT1}A_{ENZCPact} + k_{reac}A_{ENZCPinact} \tag{15.41}$$

$$\frac{dA_{ENZCinPact}}{dt} = k_{inh}A_{TT1}A_{ENZCPact} - k_{reac}A_{ENZCPinact} \tag{15.42}$$

$$\frac{dA_{ENZTT}}{dt} = k_{TTenz} - k_{TTenz}\left(1 - \frac{E_{max}C_{CP1}}{IC_{50} + C_{CP1}}\right)A_{ENZTT} \tag{15.43}$$

where all the parameters in the differential equations are explained in Fig. 15.18.

This integrated model describes the mutual DDI between CP and TT successfully at the level of enzyme kinetics as shown in Fig. 15.19 where model-predicted concentrations and individual-predicted concentrations of CP, HCP, TT, and T are adequately fitted the corresponding observed concentrations analyzed with a population PK approach with NONMEM. The induction of TT clearance caused by CP, the inhibition of CP activation by TT, and CP autoinduction involving CYP enzymes are adequately characterized with acceptable precision (RSE% $<$ 17%) and relatively small residual variability (RSE% $<$ 79%) utilizing this model.

15.5.4 Evaluation of Elimination Kinetics from Plasma Concentration–Time Data

Most drugs are eliminated through hepatic, renal, and/or biliary processes that may follow the first-order or M–M saturable kinetics. Typically, the one-, two-, and three-compartment models are used to describe plasma concentration–time profiles with the elimination of drugs from the central compartment as shown with models and schemes in Table 15.3. Several nontraditional and emerging compartmental elimination PK models are discussed in this chapter.

15.5.4.1 Elimination from a Compartment Other than the Central Compartment. If either one or two elimination pathways from the central compartment and another peripheral compartment are added to the normal scheme, the elimination rate constants will be overparameterized when solving the three-compartment PK equation. In fact, it is impossible to ascertain from drug concentrations in systemic circulation whether the model should have elimination from one, two, or three compartments. Disposition of dicumarol was molded with a three-compartment model in which elimination occurred from one of the peripheral compartment only as shown in Fig. 15.20 [19]. The transfer and elimination processes in the three-compartment open system may be represented by the following diffraction equations:

$$\frac{dA_1}{dt} = -(k_{12} + k_{13})A_1 + k_{21}A_2 + k_{21}A_3 \tag{15.44}$$

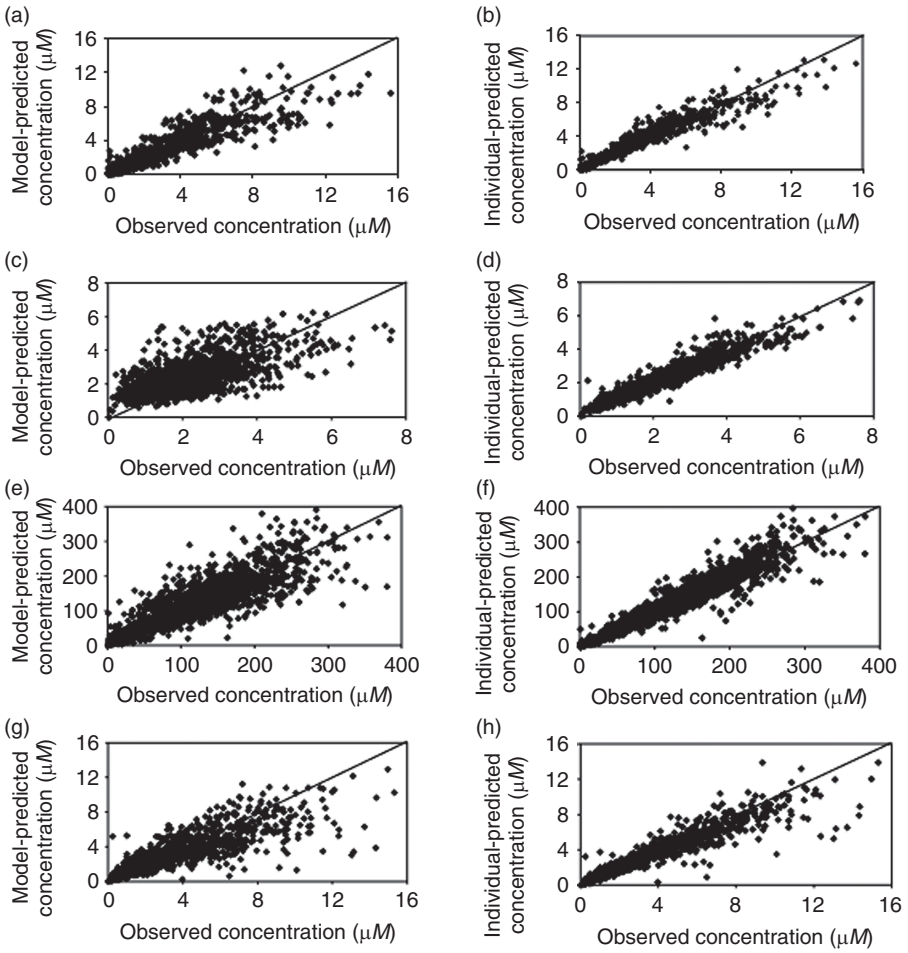

Figure 15.19 Model-predicted and individual-predicted concentrations versus the observed concentrations for thiotepa (a and b), tepa (c and d), cyclophosphamide (e and f), and 4-hydroxy-cyclophosphamide (g and h) [18].

$$\frac{dA_2}{dt} = -(k_{20} + k_{21})A_2 + k_{12}A_1 \tag{15.45}$$

$$\frac{dA_3}{dt} = -k_{31}A_3 + k_{13}A_1 \tag{15.46}$$

where A is the amount of drug in the designated compartment and k the rate constant.

By assuming that elimination occurred from the more rapidly accessible peripheral compartment, this model was used to describe the plasma concentration–time profile of dicumarol of the apparent first-order elimination rate constant decreased with increasing dose. This phenomenon is explained by the concentration-dependent inhibition of own biotransformation when the high concentrations of the drug are present in the liver and concentration-dependent protein binding of the drug, which was supported by the investigations with isolated perfused rat livers [20].

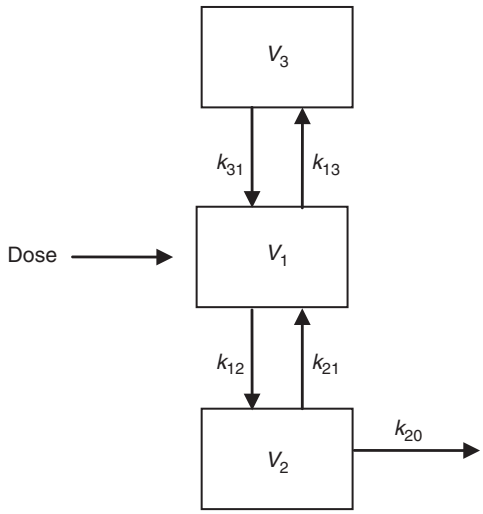

Figure 15.20 A three-compartment PK model for drugs that are eliminated from a peripheral compartment other than the central compartment.

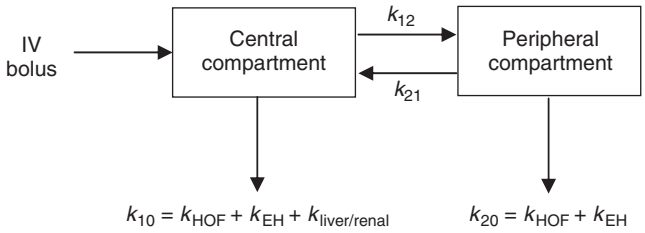

Figure 15.21 Scheme of the nontraditional two-compartment open model that elimination occurs from both the central and peripheral compartments (k_{HOF} = Hofmann elimination rate constant; k_{EH} = ester hydrolysis rate constant).

15.5.4.2 Elimination from Both Central and Peripheral Compartments. When a drug is eliminated through several pathways, including both central and peripheral compartments, traditional compartmental PK models—assuming elimination from a single central compartment—are inaccurate to assess PK data. For example, the V_{ss} value of atracurium besylate, a skeletal muscle relaxant, as underestimated for ~17–20% [21,22] when a traditional PK model was used. The nontraditional PK model was developed to fit the plasma concentration–time data of cisatracurium besylate, a cis–trans isomerism form of atracurium besylate [23]. The scheme of the nontraditional two-compartment open model is depicted in Fig. 15.21. The model can be solved by the following equations:

$$C = Ae^{-\alpha t} + Be^{-\beta t} \tag{15.47}$$

where

$$V_1 = \frac{\text{Dose}}{(A + B)} \tag{15.48}$$

$$A = \frac{\text{Dose}(k_{20} + k_{21} - \alpha)}{V_1(\beta - \alpha)} \tag{15.49}$$

$$B = \frac{\text{Dose}(k_{20} + k_{21} - \beta)}{V_1(\alpha - \beta)} \tag{15.50}$$

$$\alpha + \beta = k_{10} + k_{12} + k_{20} + k_{21} \tag{15.51}$$
$$\alpha \times \beta = (k_{10} \times k_{20}) + (k_{10} \times k_{21}) + (k_{12} \times k_{20})$$

Input rate:

$$R_{\text{input}} = C_{\text{ss}} \times Cl_{\text{total}} \tag{15.52}$$

Elimination rate:

$$R_{\text{elimination}} = (k_{10} \times A_{1\text{ss}}) + (k_{20} \times A_{2\text{ss}}) \tag{15.53}$$

where $A_{1\text{ss}}$ and $A_{2\text{ss}}$ are the amounts drug in the central and peripheral compartments, respectively, at steady state.

This model has been successfully applied to describe the PK profile of cisatracurium besylate that is eliminated through multiple pathways, including Hofmann elimination, ester hydrolysis, and liver and renal elimination [21,24]. Results from this modeling supported the idea that the major elimination pathway of cisatracurium besylate in patients was Hofmann elimination that is spontaneous degradation in plasma and tissue at normal body pH and temperature. Approximately 77% of CL of cisatracurium besylate was accounted for by Hofmann elimination, while the residual drug (23%) was accounted for by liver and renal elimination.

15.5.4.3 Nonlinear Elimination—Michaelis–Menten and Target-Mediated Drug Disposition. Saturation may occur in all drug disposition processes where enzymes, transporters, or active processes are involved in biotransformation, renal tubular secretion, and active transport and binding. These processes may be specific with respect to the drug and may have limited capacities. For these specialized processes, the use of M–M kinetics or target-mediated drug disposition (TMDD), a specific case of M–M drug disposition, or mixed-order kinetics is usually applicable. For a drug showing M–M PK, capacity limitation of drug disposition/clearance can occur in many processes, including hepatic metabolism and renal and biliary excretion of a drug. For a drug characterized by TMDD first introduced by Levy [25], the saturable disposition/clearance is controlled by the pharmacological target, such as enzymes or receptors, of the drug. The TMDD phenomenon where the temporal profile of plasma or serum drug concentrations of a drug is significantly affected due to its high affinity binding to a biological target with a large amount of drug relative to dose. Since it is difficult to obtain clinical data for target kinetics, M–M kinetics where only free or total drug concentrations in a biological fluid are measured has been applied to the TMDD

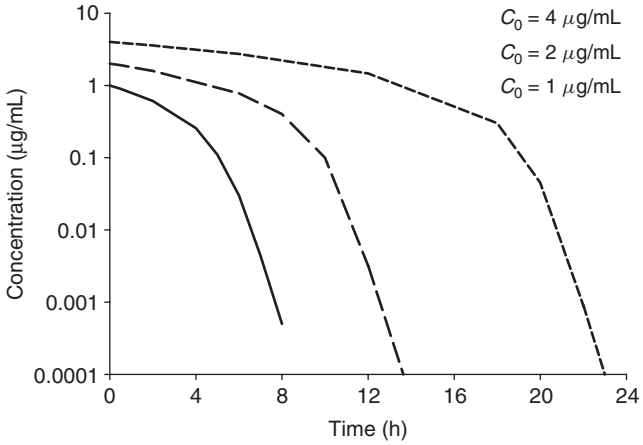

Figure 15.22 Semilogarithmic scale concentration–time profile simulated from Michaelis–Menten model with $V_m = 0.22$, $K_m = 0.1$, and $C_0 = 1$, 2, and 4 μg/mL.

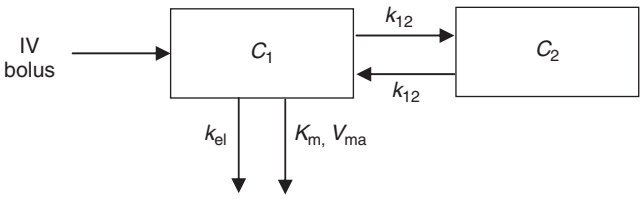

Figure 15.23 Scheme of two-compartment Michaelis–Menten model.

system with less precision. M–M and TMDD models have been used to characterize large molecular weight drugs such as monoclonal antibodies and some small molecular weight drugs such as angiotensin-converting enzyme (ACE) inhibitors [26], an aldose reductase inhibitor imirestat [27], and warfarin [28].

The typical semilogarithmic concentration–time profile of a drug fitting an M–M or TMDD model (Fig. 15.22) appears to be nonlinear with a fast elimination rate at the low dose and a slow clearance rate at the high dose. Depending on the distribution and elimination rates, some drugs with the M–M characteristics may show linear PK or the combination of linear and nonlinear PK initially after administration. The structure of a two-compartment M–M model is shown in Fig. 15.23. For IV bolus injection, drug in the central compartment (C_1) is eliminated from the system by the combination of a first-order rate constant and a saturable process described by the M–M equation. The initial conditions and model equations are as follows:

Initial conditions:

$$C_1(t) = 0, \qquad \text{for } t < t_D \tag{15.54}$$

$$C_2(t) = 0, \qquad \text{for } t \leq t_D \tag{15.55}$$

$$C_1(t_D) = \frac{D}{V}, \quad \text{for single dose} \tag{15.56}$$

$$C_1(t_{D_1}) = C_1^{(1)}(t_{D_1}) = \frac{D_1}{V}, \quad \text{for the first dose of multiple doses} \tag{15.57}$$

$$C_1(t_{D_n}) = C_1^{(n)}(t_{D_n}) = C_1^{(n-1)} + \frac{D_n}{V}, \quad \text{for multiple doses} \tag{15.58}$$

Model equations:

$$\frac{dC_1}{dt} = -\frac{\left(\frac{V_{max}}{V}\right)C_1}{K_m + C_1} - (k_{12} + k_{el})C_1 + k_{21}C_2 \tag{15.59}$$

$$\frac{dC_2}{dt} = k_{21}C_1 - k_{21}C_2 \tag{15.60}$$

where C_1 and C_2 denote free drug concentrations in the central and peripheral compartments, respectively, V is the volume distribution of the central compartment, k_{12}, k_{21}, and k_{el} are the first-order rate constants, K_m is the M–M constant, and V_m is the maximum elimination rate.

For TMDD, free drug in the central compartment (C_1) binds to its free target (R) at a second-order rate constant (k_{on}), forming a drug–target complex (RC_1), which can either be internalized and degenerated at a first-order rate (k_{int}) or dissociate at a first-order rate (k_{off}). The unbound drug can also be removed from the central compartment by a first-order elimination pathway (k_{el}) and distributed to the peripheral compartment (C_2). The targets are formed with a zero-order rate constant (k_{form}) and are degenerated with a first-order rate constant (k_{deg}). The structure of the general PK model of TMDD is presented in Fig. 15.24 and the equations combined with linear and TMDD elimination and IV bolus infusion are as follows:

$$\frac{dC_1}{dt} = \ln(t) - (k_{el} + k_{12})C_1 + k_{21}C_2 - k_{on}R \cdot C_1 + k_{off}RC_1 \tag{15.61}$$

$$\frac{dC_2}{dt} = k_{21}C_1 - k_{21}C_2 \tag{15.62}$$

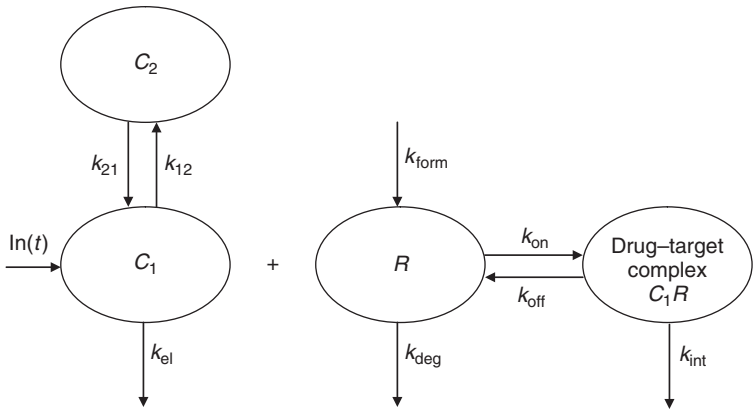

Figure 15.24 Scheme of two-compartment target-mediated drug disposition model.

$$\frac{dR}{dt} = k_{form} - k_{deg}R - k_{on}R \cdot C_1 + k_{off}RC_1 \tag{15.63}$$

$$\frac{dRC_1}{dt} = k_{on}R \cdot C_1 - (k_{int} + k_{off})RC_1 \tag{15.64}$$

Before applying the TMDD model to a specific drug, one should understand the underlying biological processes of drug binding to the target(s). The model discussed above can only be applied to the simple and specific drug–target binding process of one drug molecule to one target molecule. The drug–target binding occurs only in the central but not in the peripheral compartment. Free target formation and degeneration rates are independent of the drug and unbound target concentrations. Unbound drug distributes to peripheral compartment linearly. After internalizing, the bound drug will release from the drug–target complex so that the targets become free again. Recycling of the free target is not included in the elimination process of the drug–target complex. If a drug–target complex disposition deviates from the processes discussed here, the TMDD model should be modified so that an appropriate model can be used to characterize the PK of the drug.

Drug-binding microconstants (k_{on} and k_{off}) included in the TMDD model are sometimes difficult to estimate from routine clinical studies due to the much larger timescale of the concentration measurements than the timescale of the binding process unless there are extensive data in the transition phase. In this situation, the full TMDD model becomes overparameterized and the fit of the model to the available data becomes unstable. Approximations of the TMDD disposition model such as quasi-equilibrium (QE) [29], quasi-steady-state (QSS) [30], and M–M [29] approximations were further studied by several researchers to help solve the full TMDD model with certain conditions.

When the binding of drug to free receptor and dissociation of the drug–receptor complex are of several orders of magnitude faster than the other drug distribution and elimination processes, equilibrium between the binding and dissociation is reached instantly with unidentifiable k_{on} and k_{off}. As a consequence, QE approximation is suggested based on the following assumption [29]:

$$k_{on}R \cdot C_1 = k_{off}RC_1 \tag{15.65}$$

$$\frac{R \cdot C_1}{RC_1} = \frac{k_{off}}{k_{on}} \equiv K_D \tag{15.66}$$

where K_D represents the equilibrium dissociation constant. With this additional equation to the four full TMDD equations, four unknowns in the TMDD model will be easily resolved. Furthermore, the free drug and target concentrations in the central compartment are shown as follows:

$$C_1 = \frac{1}{2}\left[(C_{tot} - R_{tot} - K_D) + \sqrt{(C_{tot} - R_{tot} - K_D)^2 + 4K_DC_{tot}}\right] \tag{15.67}$$

$$RC_1 = \frac{R_{tot}C_1}{K_D + C} \tag{15.68}$$

In which, the total concentrations of the drug and target are as follows:

$$C_{\text{tot}} = C + RC_1 \tag{15.69}$$

$$R_{\text{tot}} = R + RC_1 \tag{15.70}$$

When the binding of drug to free receptor and dissociation of the drug–receptor complex are not much faster than drug elimination process, the rate of elimination of the complex is not negligible compared to the dissociation rate. In this case, QE approximation may not be valid. In this case, the QSS assumption that the binding rate is balanced by the sum of the dissociation and internalization rate can be applied to drug–target disposition [29]:

$$k_{\text{on}} R \cdot C_1 = (k_{\text{int}} + k_{\text{off}}) RC_1 \tag{15.71}$$

$$\frac{R \cdot C_1}{RC_1} = \frac{k_{\text{int}} + k_{\text{off}}}{k_{\text{on}}} = K_{\text{D}} + \frac{k_{\text{int}}}{k_{\text{on}}} = K_{\text{SS}} \tag{15.72}$$

$$C_1 = \frac{1}{2}\left[(C_{\text{tot}} - R_{\text{tot}} - K_{\text{SS}}) + \sqrt{(C_{\text{tot}} - R_{\text{tot}} - K_{\text{SS}})^2 + 4K_{\text{SS}}C_{\text{tot}}}\right] \tag{15.73}$$

$$RC_1 = \frac{R_{\text{tot}}C_1}{K_{\text{SS}} + C} \tag{15.74}$$

where K_{SS} denotes the steady-state constant. The QSS approximation can be applied to the drug with fast drug–target association and dissociation as well as fast internalization of the drug–target complex.

When the free drug concentration is large relative to the total target concentration, the time derivatives of the free and total drug concentrations are similar where M–M approximation can be used to solve the full TMDD model [29]. Both M–M and TMDD models are applied to the elimination process with capacity limitation and both systems are saturated at high dose. However, the M–M model exhibits linear parallel clearance at low doses. On the other hand, a very rapid drop and long terminal phase occur in TMDD systems [31]. The rapid decrease in drug concentrations reflects the loss of drug in the central compartment by rapid binding to the targets at low doses. The processes of drug elimination controlled by the rates of k_{12}, k_{21}, K_{D}, k_{el}, and k_{int} as well as the initial free target concentration attribute to the relatively long terminal phase.

15.6 SUMMARY

The PK of unchanged drug and the pseudo-PK parameters of TRA must be estimated in human ADME studies. With multiple PK samples collected in plasma and excreta, the PK parameters that represent the extent of a drug in or clearance from the circulation system are readily determined using a noncompartment approach that can be executed quickly in routine and traditional PK data analysis without assumption on disposition of drug in the body. Mechanism- or compartment-based PK models contain specific expression to characterize, in a quantitative manner, processes on the causal path from absorption, distribution, and metabolism to elimination. Data analysis using modeling

will provide information on not only the extent of a drug in the body but also the rate of a drug transferring through different parts of the body. Pooling PK data from a human ADME together with the data from the other studies of the same molecule can help scientists build a more robust population PK model, which can be used in interpreting or predicting the underlying physiological or pathological processes that drugs act on and for optimizing therapy with drugs that have a complex disposition.

REFERENCES

1. Christopher LJ, Hong H, Vakkalagadda BJ, *et al*. Metabolism and disposition of [^{14}C]BMS-690514, an ErbB/vascular endothelial growth factor receptor inhibitor, after oral administration to humans. Drug Metab Dispos 2010;38(11):2049–2059.
2. Beumer JH, Beijnen JH, Schellens JH. Mass balance studies, with a focus on anticancer drugs. Clin Pharmacokinet 2006;45(1):33–58.
3. Roffey SJ, Obach RS, Gedge JI, *et al*. What is the objective of the mass balance study? A retrospective analysis of data in animal and human excretion studies employing radiolabeled drugs. Drug Metab Rev 2007;39(1):17–43.
4. Tucker GT. Measurement of the renal clearance of drugs. Br J Clin Pharmacol 1981;12(6):761–770.
5. Martin BK. Drug urinary excretion data—some aspects concerning the interpretation. Br J Pharmacol Chemother 1967;29(2):181–193.
6. Gabrielsson J, Weiner D. Pharmacokinetic and pharmacodynamic data analysis: concepts and applications. 4th ed. Sweden: Swedish Pharmaceutical Press, Kristianstads Boktryckeri AB; 2006
7. Perez-Ruixo JJ, Piotrovskij V, Zhang S, *et al*. Population pharmacokinetics of tipifarnib in healthy subjects and adult cancer patients. Br J Clin Pharmacol 2006;62(1):81–96.
8. Wagner JG, Nelson E. Kinetic analysis of blood levels and urinary excretion in the absorptive phase after single doses of drug. J Pharm Sci 1964;53:1392–1403.
9. Wagner JG, Nelson E. Percent absorbed time plots derived from blood level and/or urinary excretion data. J Pharm Sci 1963;52:610–611.
10. Loo JC, Riegelman S. New method for calculating the intrinsic absorption rate of drugs. J Pharm Sci 1968;57(6):918–928.
11. Debord J, Risco E, Harel M, *et al*. Application of a gamma model of absorption to oral cyclosporin. Clin Pharmacokinet 2001;40(5):375–382.
12. Suttle AB, Pollack GM, Brouwer KL. Use of a pharmacokinetic model incorporating discontinuous gastrointestinal absorption to examine the occurrence of double peaks in oral concentration-time profiles. Pharm Res 1992;9(3):350–356.
13. Röshammar D, Hai TN, Friberg Hietala S, *et al*. Pharmacokinetics of piperaquine after repeated oral administration of the antimalarial combination CV8 in 12 healthy male subjects. Eur J Clin Pharmacol 2006;62(5):335–341.
14. Ezzet F, Krishna G, Wexler DB, *et al*. A population pharmacokinetic model that describes multiple peaks due to enterohepatic recirculation of ezetimibe. Clin Ther 2001;23(6):871–885.
15. Bundgaard C, Jørgensen M, Larsen F. Pharmacokinetic modelling of blood-brain barrier transport of escitalopram in rats. Biopharm Drug Dispos 2007;28(7):349–360.
16. Benet LZ. General treatment of linear mammillary models with elimination from any compartment as used in pharmacokinetics. J Pharm Sci 1972;61(4):536–541.
17. Tan B, Naik H, Jang IJ, *et al*. Population pharmacokinetics of artesunate and dihydroartemisinin following single- and multiple-dosing of oral artesunate in healthy subjects. Malar J 2009;8:304.

18. de Jonge ME, Huitema AD, Rodenhuis S, *et al*. Integrated population pharmacokinetic model of both cyclophosphamide and thiotepa suggesting a mutual drug-drug interaction. J Pharmacokinet Pharmacodyn 2004;31(2):135–156.
19. Nagashima R, Levy G, Sarcione EJ. Comparative pharmacokinetics of coumarin anticoagulants. 3. Factors affecting the distribution and elimination of bishydroxycoumarin (BHC) in isolated liver perfusion studies. J Pharm Sci 1968;57(11):1881–1888.
20. Nagashima R, Levy G, O'Reilly RA. Comparative pharmacokinetics of coumarin anticoagulants. IV. Application of a three-compartmental model to the analysis of the dose-dependent kinetics of bishydroxycoumarin elimination. J Pharm Sci 1968;57(11):1888–1895.
21. Lien CA, Schmith VD, Belmont MR, *et al*. Pharmacokinetics of cisatracurium in patients receiving nitrous oxide/opioid/barbiturate anesthesia. Anesthesiology 1996;84(2):300–308.
22. Kisor DF, Schmith VD, Wargin WA, *et al*. Importance of the organ-independent elimination of cisatracurium. Anesth Analg 1996;83(5):1065–1071.
23. Fisher DM, Canfell PC, Fahey MR, *et al*. Elimination of atracurium in humans: contribution of Hofmann elimination and ester hydrolysis versus organ-based elimination. Anesthesiology 1986;65(1):6–12.
24. Fisher DM, Rosen JI. A pharmacokinetic explanation for increasing recovery time following larger or repeated doses of nondepolarizing muscle relaxants. Anesthesiology 1986;65(3):286–291.
25. Levy G. Pharmacologic target-mediated drug disposition. Clin Pharmacol Ther 1994;56(3):248–252.
26. Till AE, Gomez HJ, Hichens M, *et al*. Pharmacokinetics of repeated single oral doses of enalapril maleate (MK-421) in normal volunteers. Biopharm Drug Dispos 1984;5(3):273–280.
27. Brazzell RK, Mayer PR, Dobbs R, *et al*. Dose-dependent pharmacokinetics of the aldose reductase inhibitor imirestat in man. Pharm Res 1991;8(1):112–118.
28. Cheung WK, Levy G. Comparative pharmacokinetics of coumarin anticoagulants. XLIX: Nonlinear tissue distribution of S-warfarin in rats. J Pharm Sci 1989;78(7):541–546.
29. Mager DE, Krzyzanski W. Quasi-equilibrium pharmacokinetic model for drugs exhibiting target-mediated drug disposition. Pharm Res 2005;22(10):1589–1596.
30. Gibiansky L, Gibiansky E, Kakkar T, *et al*. Approximations of the target-mediated drug disposition model and identifiability of model parameters. J Pharmacokinet Pharmacodyn 2008;35(5):573–591.
31. Yan X, Mager DE, Krzyzanski W. Selection between Michaelis-Menten and target-mediated drug disposition pharmacokinetic models. J Pharmacokinet Pharmacodyn 2010;37(1):25–47.